Research in Astronomy and Astrophysics, 22:115009 (10pp), 2022 November https://doi.org/10.1088/1674-4527/ac91bd

Inter-correlation between Sunspot Oscillations and Their Internal Structures

Libo Fu[1], Zizhan Zhu[1], Ding Yuan[1], Jiaoyang Wang[1], Song Feng[2], and Sergey Anfinogentov[3]
[1] Institute of Space Science and Applied Technology, Harbin Institute of Technology, Shenzhen 518055, China; yuanding@hit.edu.cn
[2] Faculty of Information Engineering and Automation, Kunming University of Science and Technology, Kunming 650500, China
[3] Institute of Solar-Terrestrial Physics SB RAS, Lermontov st. 126a, 664033, Irkutsk, Russia
Received 2022 July 11; revised 2022 September 6; accepted 2022 September 9; published 2022 October 19

Abstract

Three- and five-minute oscillations are commonly observed in any sunspot. Because they are modulated by the internal thermal and magnetic structures of a sunspot, they could be used as an effective tool for researching sunspot seismology. In this paper, we investigate the properties of oscillations in sunspot groups with varying sizes and magnetic fields, and aim to establish the relationships between sunspot oscillations and its internal structure comparatively. We selected three groups of the unipolar sunspot with approximately axial-symmetric magnetic field and calculated their Fourier spectra based on the ultraviolet/extreme ultraviolet emission intensity variations recorded by the Solar Dynamics Observatory/Atmospheric Imaging Assembly. We found that the distribution of three-minute oscillation is defined by the joint effect of diverging magnetic field and the stratification of the sunspot atmosphere. Its distribution could be modified by any invading magnetic structures in the umbra. In contrast, the five-minute oscillations are more prominent in small spots, implying that five-minute oscillation is very closely connected with umbral dynamics.

Key words: (Sun:) sunspots – Sun: oscillations – methods: data analysis

1. Introduction

Waves and oscillations are commonly found in sunspots and could reveal the internal structure of sunspots (Khomenko & Collados 2015; Yuan et al. 2016). The spatial distribution of oscillatory signals could provide an effective probe of the magnetic field of a sunspot (Khomenko & Collados 2006; Yuan et al. 2014a). Sunspot oscillations are classified into three-minute umbral wave and five-minute running penumbral waves at multiple layers of the sunspot atmosphere (Bogdan & Judge 2006; Yuan et al. 2014b). They are both considered as slow-mode magnetoacoustic waves propagating along the magnetic field (De Moortel et al. 2002; Sych & Nakariakov 2014). Because they perturb the plasma density (or pressure), these waves are frequently detected as emission intensity variations at various UV/EUV bandpasses (Botha et al. 2011; Yuan & Walsh 2016). Therehence, sunspot oscillations could be used to diagnose the temperature and magnetic field structure of a sunspot.

Although sunspot oscillations were traditionally studied case by case, no statistical and comparative study was conducted. In this study, we compare the characteristics of sunspot oscillations with different thermodynamic structures and magnetic fields, and aim to establish the empirical correlations between the internal structure of a sunspot and the properties of the oscillatory signals. The thermodynamic structure of a sunspot describes the spatial distribution of the macroscopic parameters of sunspot plasma, such as density, temperature, pressure, ionization level, thermal conduction, viscosity, among others. This would enable the possibility of using sunspot oscillations to diagnose the internal structure of sunspots.

This paper is organized as follows. Section 2 introduces the instrumentation and data analysis used in this study. Section 3 discusses the spatial distributions of properties of sunspot oscillations. Section 4 presents the conclusion and discussion.

2. Observation and Method

2.1. Data Selection and Calibration

In this study, we selected 15 unipolar (or alpha) sunspots of various sizes for statistical comparison. The coordinates, start time of observation, classification, and size are listed in Table 1. A sunspot with diameter between 5″ and 15″ is classified as a small-sized spot, whereas the medium- and large-sized spots have a diameter of 30″–40″ and 50″–60″, respectively.

For each sunspot, we used continuous observations of four UV/EUV channels of SDO/AIA: 1600 Å, 1700 Å, 304 Å, and 171 Å. These channels could reveal the dynamics in the sunspot atmosphere from the photosphere and chromosphere to the corona. The AIA 1600 Å is the C IV spectral line, whose radiation mainly originates from the transition region and the upper photosphere. The AIA 1700 Å is the C IV spectral line near the continuum, which originates from the temperature minimum and the photosphere. The AIA 304 Å is the He II spectral line, which originates from the chromosphere and the

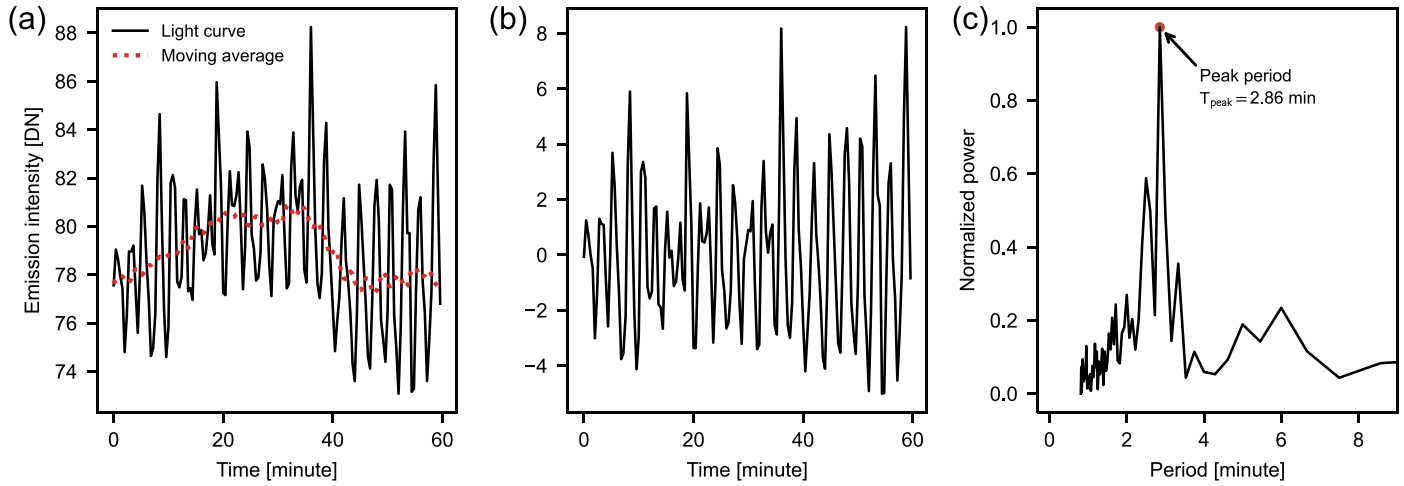

Figure 1. (a) Light curve of an example pixel in SDO/AIA 1600 Å dataset and its 10-minute moving average curve, the start time is 2011 October 10 17:59 UT. (b) De-trended light curve. (c) Normalized Fourier power spectrum of the de-trended light curve.

Table 1
Metrics of Selected Sunspots

NOAA	Location	Start Time (UT)	Sunspot Classification[a]	Approximate Diameter	Size (S/M/L)
11115	(−4″, 541″)	2010-10-20 22:30	Hsx	30″	M
11312	(−2″, 290″)	2011-10-10 18:00	Hsx	60″	L
11353	(− 5″, 100″)	2011-11-23 9:00	Hsx	5″	S
11445	(−5″, 260″)	2012-3-29 13:00	Hsx	35″	M
11528	(−5″, 200″)	2012-7-28 18:00	Cso	15″	S
11537	(−5″, 110″)	2012-8-6 17:00	Hsx	15″	S
11546	(−5″, 150″)	2012-8-22 9:00	Hsx	15″	S
11569	(−5″, −300″)	2012-9-15 17:00	Eac	55″	L
11579	(−5″, −270″)	2012-9-30 11:00	Cso	60″	L
11591	(0″, 40″)	2012-10-18 9:00	Dso	50″	L
11665	(−5″, 290″)	2013-2-3 20:00	Hax	55″	L
11801	(−5″, 240″)	2013-7-29 8:00	Hsx	15″	S
11899	(−5″, 55″)	2013-11-18 16:00	Cko	60″	L
12107	(−5″, −370″)	2014-7-5 22:00	Dko	30″	M
12186	(−5″, −430″)	2014-10-13 16:00	Cso	35″	M

Note.
[a] In this paper, we use the three-component McIntosh classification to represent the sunspot category. The three components represent the modified Zurich class, penumbra of the largest spot, distribution of sunspots (More details in McIntosh 1990).

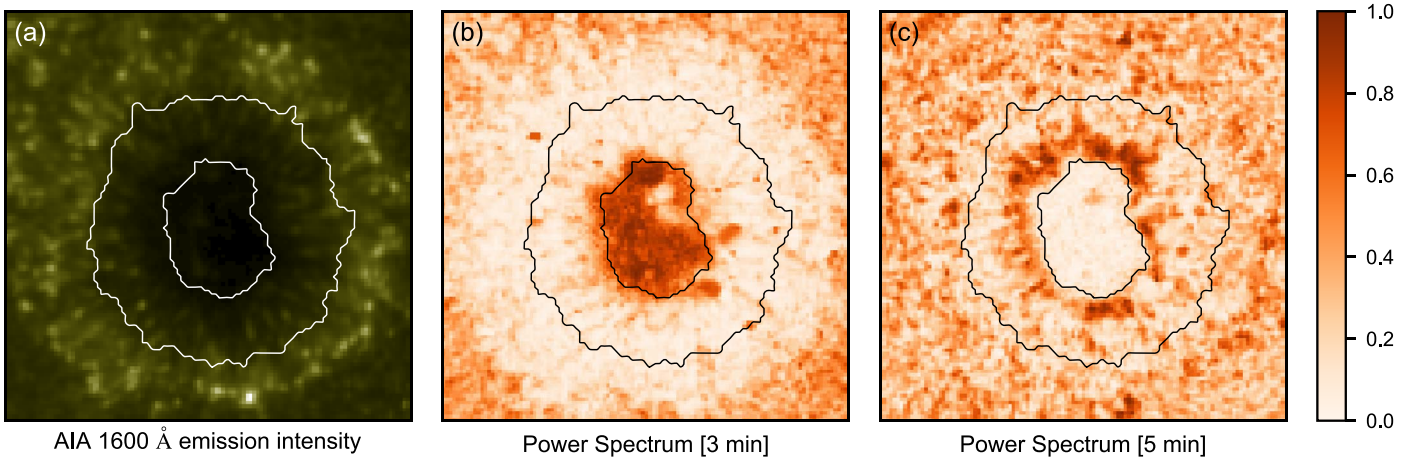

Figure 2. (a) SDO/AIA 1600 Å observation of the active region AR11312, recorded at 2011 October 10 17:59 UT. Two closed curves indicate the umbral and penumbral boundaries, determined with the HMI continuum intensity image. (b), (c) Normalized narrowband spatial distribution averaged between 1–4 minutes and 4–6 minutes, denoted as P_3 and P_5, respectively.

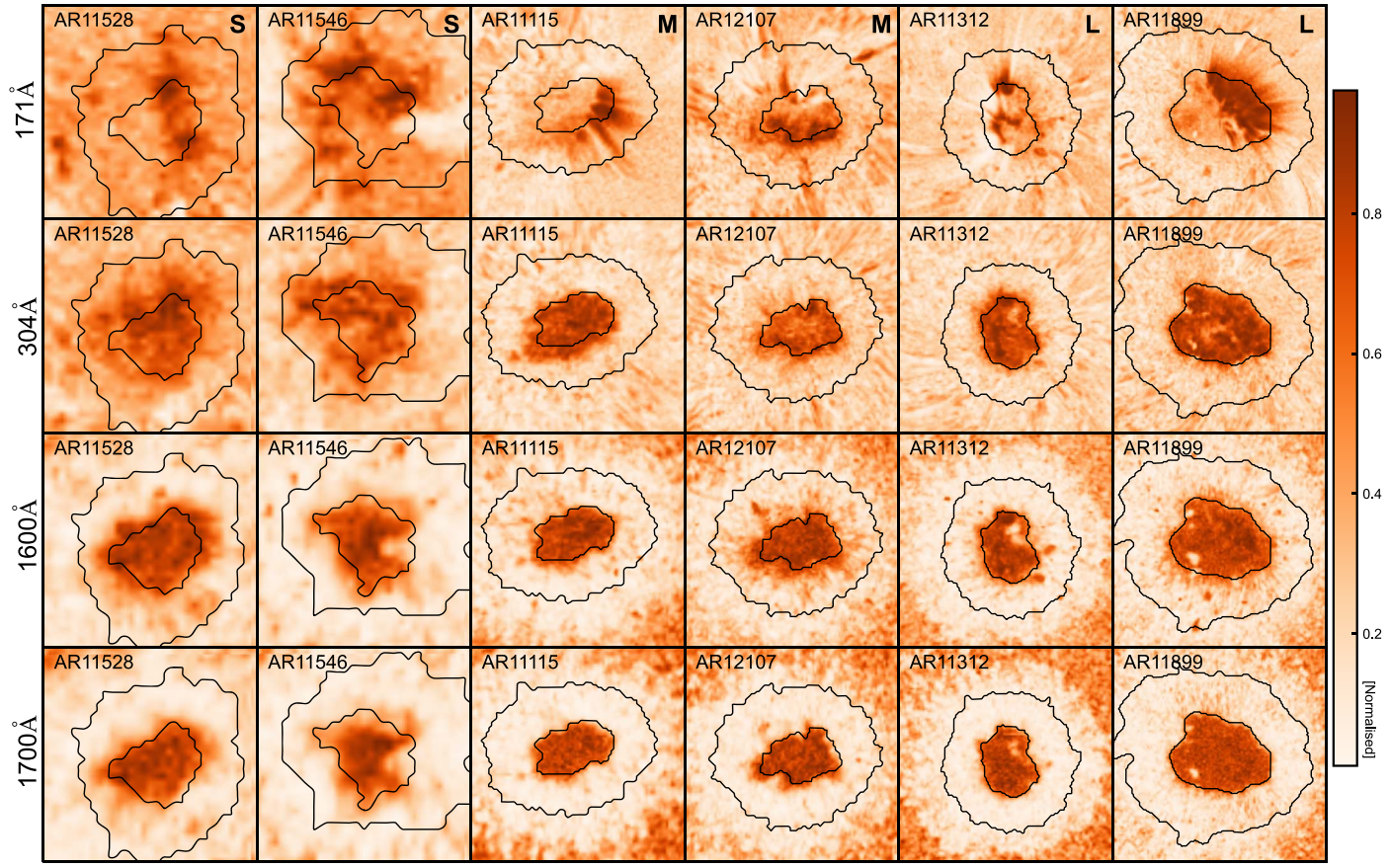

Figure 3. Spatial distribution of three-minute oscillations P_3 at multiple bandpasses of sunspots, observing four bands of AIA. The first two columns for small-sized sunspots, the third and fourth columns for medium-sized sunspots, and the last two columns for large-sized sunspots.

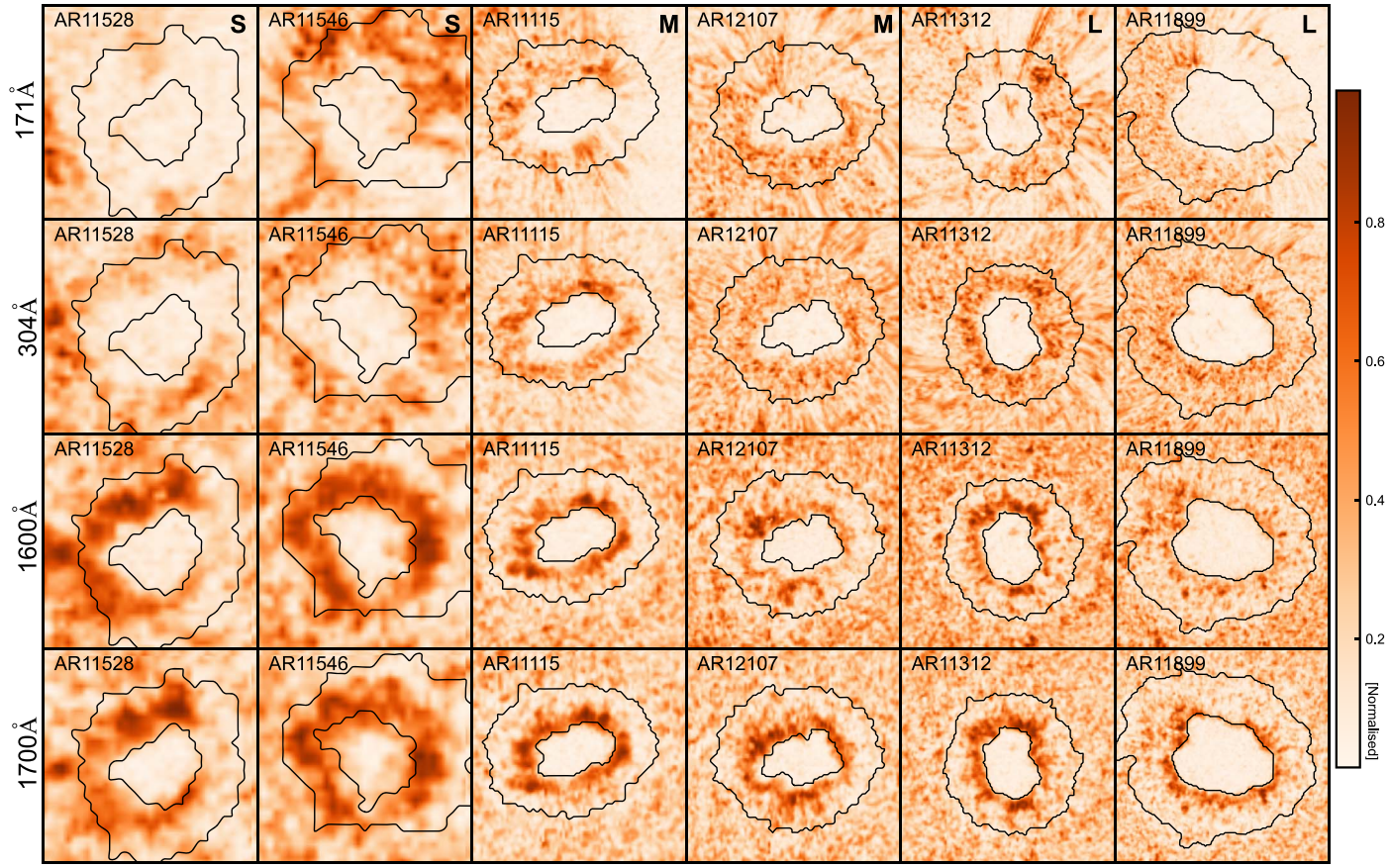

Figure 4. Spatial distribution of five-minute oscillations P_5 at multiple bandpasses of sunspots.

transition region. The AIA 171 Å originates from the quiet corona and the upper transition region (Lemen et al. 2011).

The channels of 171 Å and 304 Å have a cadence of 12 s, whereas the channels of 1600 Å and 1700 Å have a cadence of 24 s. Each dataset has a one-hour continuous observation with spatial resolution of 1.″2.

The data were calibrated with the standard routine (aia_prep.pro) provided by the SolarSoftWare. This step removed the hot pixels in the CCD (Charge-Coupled Device) and subtracted the dark currents. Then, the flat field was corrected, and each image was normalized by its exposure time. To track the sunspot, we followed the differential rotation of the Sun. Thereafter, the one-hour observational data were aligned to the sub-pixel accuracy. To study the association between sunspot magnetic fields in various sizes of sunspots, we have used the Vector Magnetic Field from HMI/SDO (Scherrer et al. 2012), which computed every 12 minutes (720 s).

2.2. Periodicity Analysis and Peak Period Distribution

To calculate the Fourier spectrum, we extracted the time series (or light curve) of the emission intensity for each pixel. Then, each time series was de-trended by removing a moving average of a 10-minute window, and was analyzed by Fourier transform. The time series of an exemplary pixel in the SDO/AIA 1600 Å and its processing procedure is illustrated in Figure 1. This analysis was applied pixel-by-pixel to each dataset. Next, each dataset was transformed into Fourier space.

To calculate the power spectra for the umbral and penumbral oscillations, we calculated the average narrowband power distribution in the range of three and five minutes, which are denoted with P_3 and P_5, respectively. The period intervals were set to 1–4 minutes and 4–6 minutes, respectively. The average power spectrum is illustrated in Figures 2(b) and (c). The spatial structures of three- and five-minute oscillations for the 1600 Å, 1700 Å, 304 Å, and 171 Å bandpasses are visualized in Figures 3 and 4, respectively.

The peak period $T_{\rm peak}$ is the period corresponding to the strongest power in spectrogram. After obtaining the spectrum for each pixel point of the sunspot data separately, the period corresponding to the maximum power value in the spectrum plot is defined as the peak period for each pixel, see Figure 1.

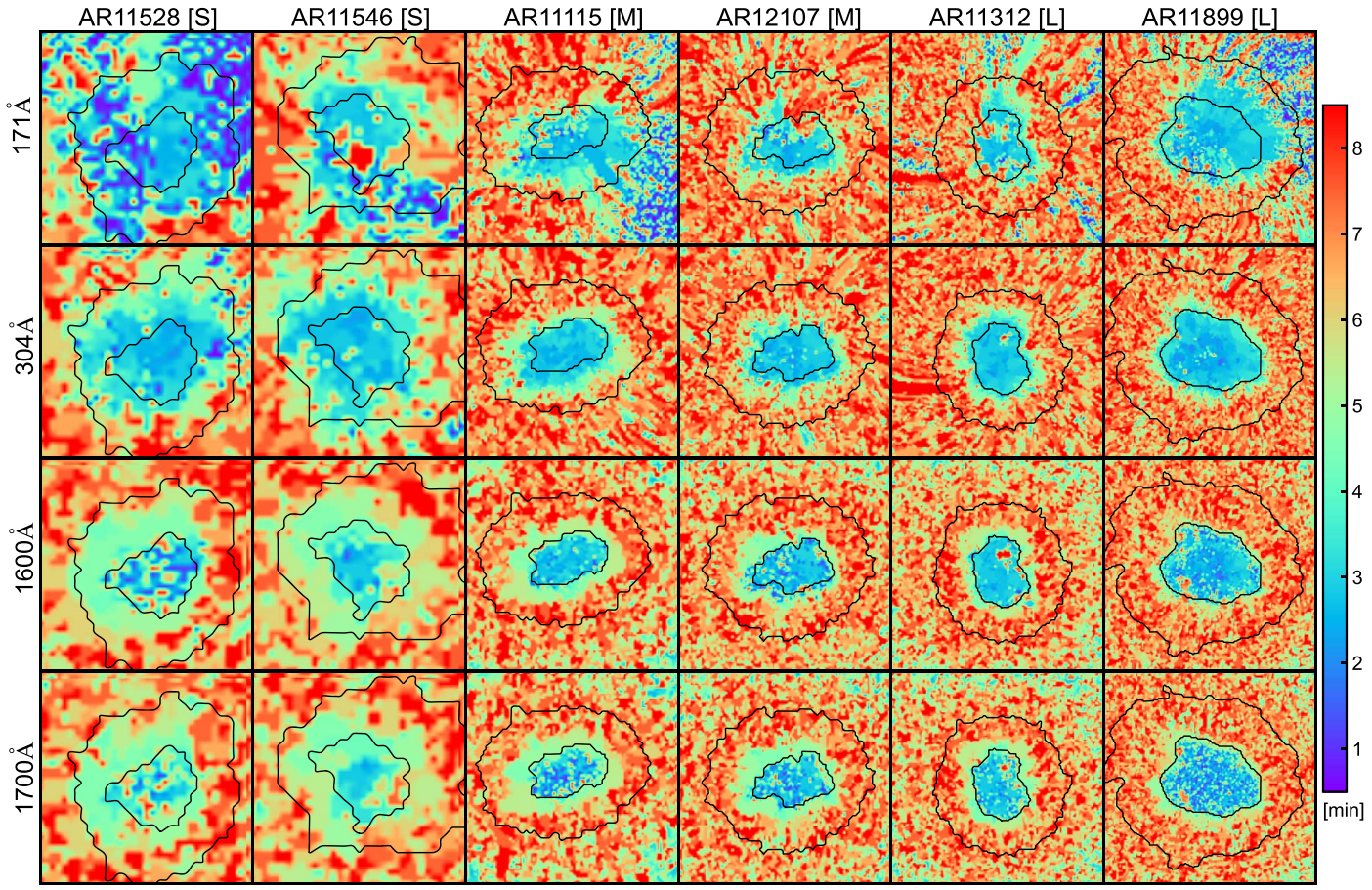

Figure 5. Spatial distribution of the peak period $T_{\rm peak}$ of the intensity oscillation in the sunspot region.

2.3. Profiles of Three-minute and Five-minute Oscillation in a Sunspot

In this paper, sunspot groups of different sizes are selected to reduce the differences due to AIA resolution. To obtain the spatial distribution (or profile) of sunspot oscillations, we interpolated the averaged narrowband spatial distribution and magnetic field strength over a slit across the sunspot center. The center of the sunspot umbra to the penumbra boundary in the selected image is used as a slicing slit, i.e., the circle is divided evenly into 16 parts. To reduce the error introduced by the non-circular shape of a sunspot, we took the average value over 16 slits. Each slit was 22.°4 apart from its neighbor in the polar coordinate with origin at the sunspot center. The mean value and standard deviation of the power profiles along 16 slits was used as the profile and its uncertainty.

To compare the power profile of sunspots with various sizes, we normalized the geometry of a sunspot to its radius (Figures 7 and 8). This step was also applied to the properties of the magnetic field (Figure 6).

3. Results

3.1. Power Distribution Analysis

To visualize the performance of the observed oscillatory motion in sunspots in various bandpasses, Figure 3 shows six selected sunspots with different sizes. Each sunspot sample was interpolated to ensure a consistent image size for the sample of sunspots.

It could seen that in the 1600 Å, 1700 Å, and 304 Å bandpasses, the three-minute oscillation is mainly distributed in the umbra, revealing the structure of the sunspot umbra. In contrast, in the 171 Å, the 3 minute-oscillation follows the coronal loop structures, revealing its nature of a propagating wave.

The 3-minute power distributions of small-sized sunspots have irregular shapes, whereas those of the medium- and large-sized spots have a more circular shape. The difference is that the large-sized sunspots reveal better fine structures in the power distribution because larger sunspots are more visible in more detail than smaller sunspots due to spatial resolution. It also could show that with the increase in the formation height

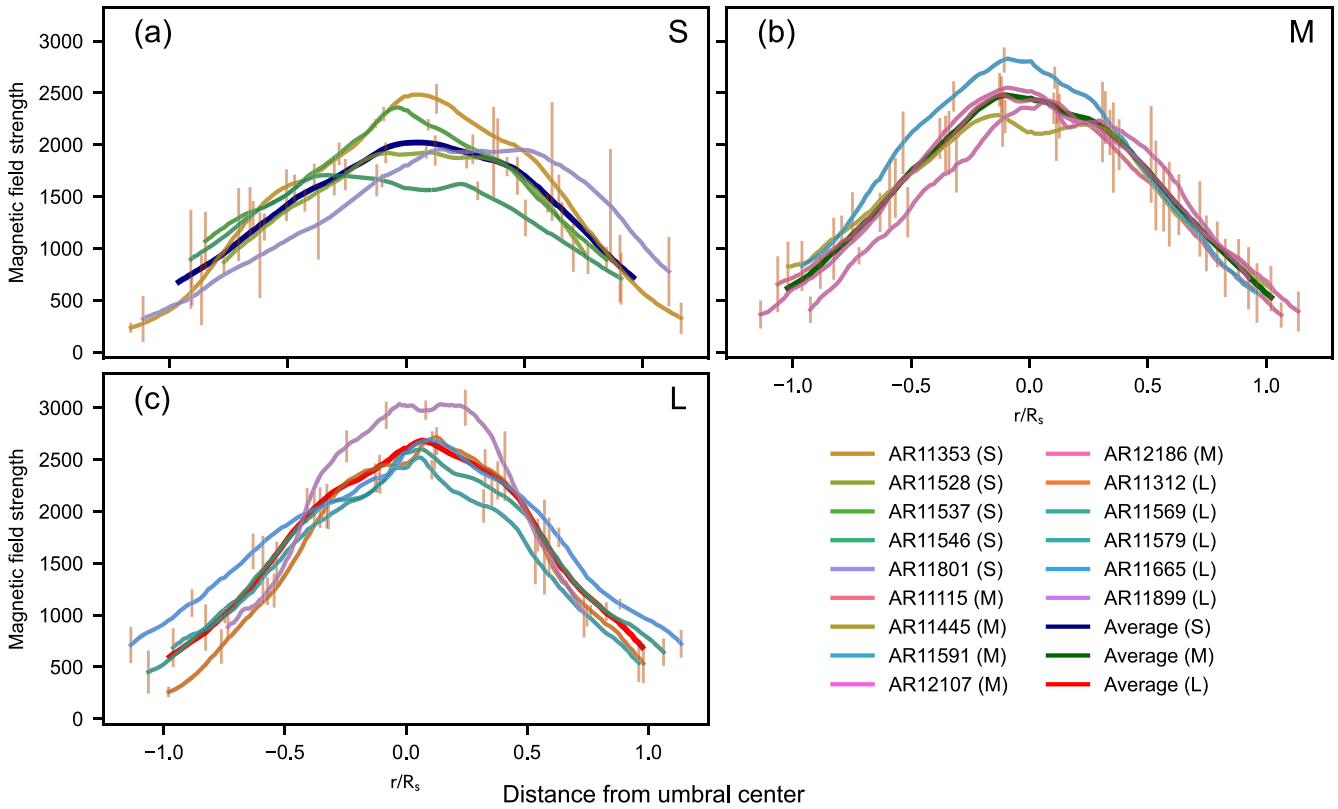

Figure 6. Magnetic field intensity slice diagram, from SDO/HMI. The horizontal coordinate measures the distance from the center of the sunspot. The value indicates the scale in units of the sunspot diameter. The vertical coordinate is the value of magnetic field strength. The vertical bar is the standard error.

of the AIA band passband, the area occupied by the three-minute oscillations is expanding (as shown in AR11115 and AR11312). These results are consistent with earlier results (Reznikova & Shibasaki 2012).

Figure 4 shows the five-minute power distribution of the sunspots, which is a five-minute equivalent of Figure 3. The five-minute oscillation power usually forms a ring structure around a sunspot (Kobanov et al. 2013). In small- and medium-sized sunspots, this structure is very apparent. However, in large-sized sunspots, this structure becomes very diffuse. In some large spots (e.g. AR11899), the five-minute oscillation even disappeared.

3.2. Distribution of Peak Period

Figure 5 presents the peak period distribution of six sunspots of various sizes and in multiple bandpasses. In a sunspot of any size, the umbral region is normally occupied by oscillations with peak period around three minutes, where as the penumbral region is dominated by five-minute oscillations. The 171 Å data reveal a different physics, as the five-minute oscillation could not propagate to the corona.

In the large sunspots (e.g. AR11899 and AR11312), the umbral region presents a very fine structure. The whole umbral region was filled with three-minute oscillations and many other oscillations. Numerous dot-shaped regions were filled with either one-minute oscillations, as studied in Wang et al. (2018) or five-minute oscillations. The one- and five-minute oscillations are uniformly distributed around the umbral region.

As the sunspot size increases, the range of high frequency regions with lower main peak period is larger in the sunspot region. Compared with the five minutes of $T_{\rm peak}$ spatial distribution of AIA 1600 Å, the ring structure formed by the low frequency signal in the five minutes of the $T_{\rm peak}$ spatial distribution of AIA 1700 Å is more obvious, indicating that the long period signal in the penumbral region is more significant. Focusing on sunspots of different sizes at AIA 1700 Å, it can be found that the ring structure is more evident to sunspots with larger diameters. We can also find some low frequency oscillations (as in AR11312) in large- and medium-sized sunspot umbra, the spatial structure can also find in the three-minute power distribution.

The three-minute oscillation dominates in the penumbra of AIA 304 Å images, unlike the mixed wave modes with three- and five-minute oscillations in the photosphere. In 171 Å, intensity oscillations seem to have disappeared and the signal has been dispersed. Normally, small-sized sunspots have fewer details in spatial resolution, but in fact the signal-to-noise ratio (S/N) of small spots is better, as the umbra of a spot normally

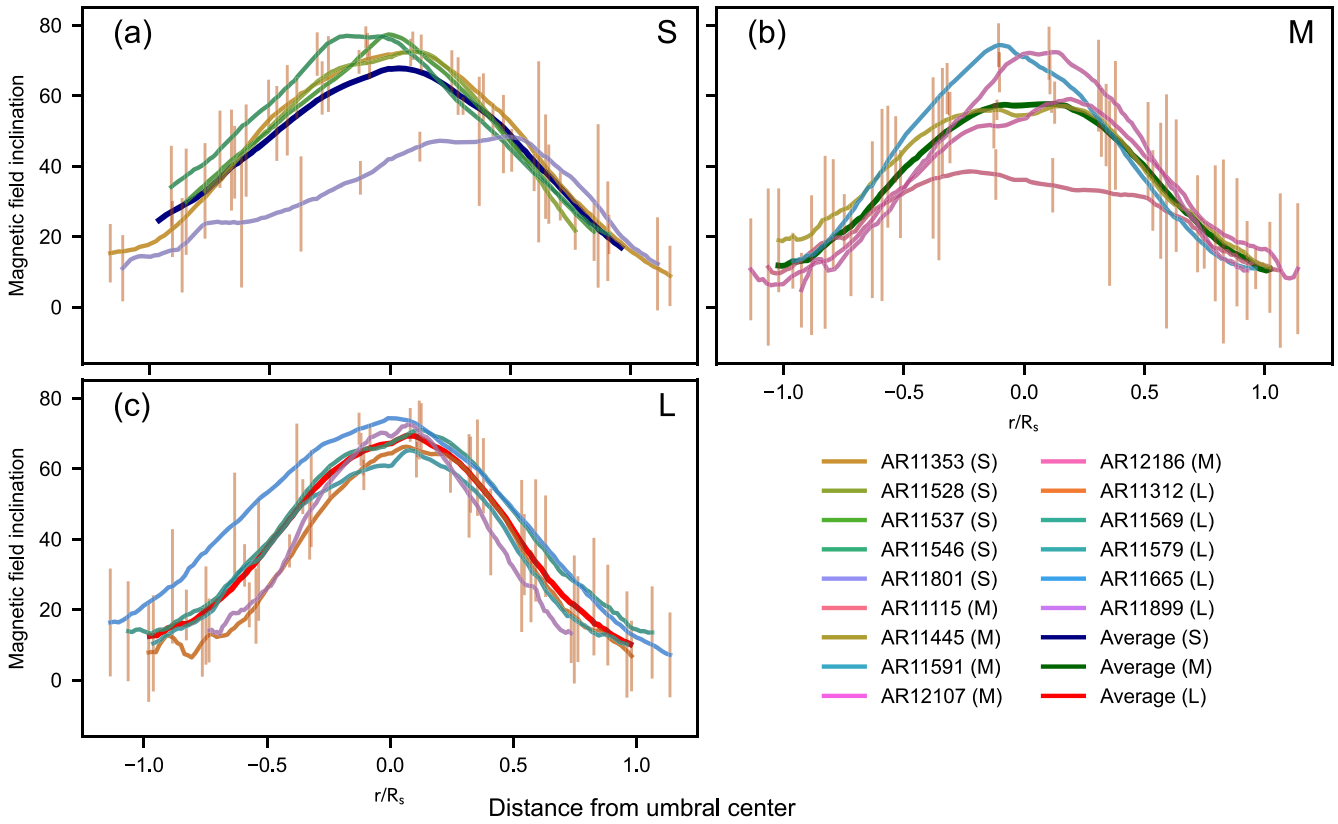

Figure 7. Magnetic field inclination slice diagram, from SDO/HMI. The vertical coordinate is inclination, limit the inclination angle to less than 90° to eliminate the effect of different magnetic poles.

darker than that of penumbra and quiet Sun region. As studied in the noise analysis of SDO/AIA (Yuan & Nakariakov 2012), the photon noise dominates in data noises, including the photon Poisson noise, compression noise, dark current noise, and despike noise, among others. The stronger emission intensity has a larger photon counts and hence a better S/N, the umbra of a small spot is relatively brighter than that of a large spot, so they have a better S/N.

Figure 5 shows the main oscillation period of sunspots with altitude, where the main oscillations of the umbra gradually change from those with a 5 minutes peak period to those with a 3 minutes period as the atmospheric altitude increases, with oscillations in the 5 minutes range dominating around sunspots. Comparison with the peak period diagram of the lower photosphere (1600 Å, 1700 Å) proves that these oscillations are still caused by the influence of the photospheric P-mode oscillations.

3.3. Relationship between Sunspot Oscillations and Its Internal Structure

Figures 6 and 7 present the slice information of the magnetic field strength and inclination, from which it can be seen that the overall magnetic field distribution of sunspots shows a bell-shaped curve, the magnetic field strength of small sunspots is 500–1000 Gauss lower than that of large sunspots, and the magnetic field in the sunspot region gradually decreases about 70° from the nearly vertical center of the penumbra to the edge of the penumbra. The larger the size of the sunspot, the more compact the magnetic field structure is. The smaller the half-peak width of the bell-shaped curve is, and the smaller the standard error is. The farther the distance from the sunspot center, the larger the standard error of the slice.

Figure 8 compared slices of sunspot power distribution P_3, all sunspot curves at 1600 Å, 1700 Å, and 304 Å are similar to the bell shape. The bell-shaped diagrams are narrower for the smaller size sunspots, which have smaller half-peak widths. Overall, the further away from the sunspot center, the smaller the sunspot size and the larger the standard error of the slice. The 171 Å slice plots exhibit no obvious pattern, and large sunspots are comparable to small sunspots in terms of error performance. Figure 9 shows the comparison of slices of sunspot P_5. All sunspot curves show a double-hump structure. The different sizes of sunspot slices in this figure show that small and large size sunspots have relatively insignificant structural changes. The amplitude of the fluctuations of medium-sized sunspot in the region of penumbra is more

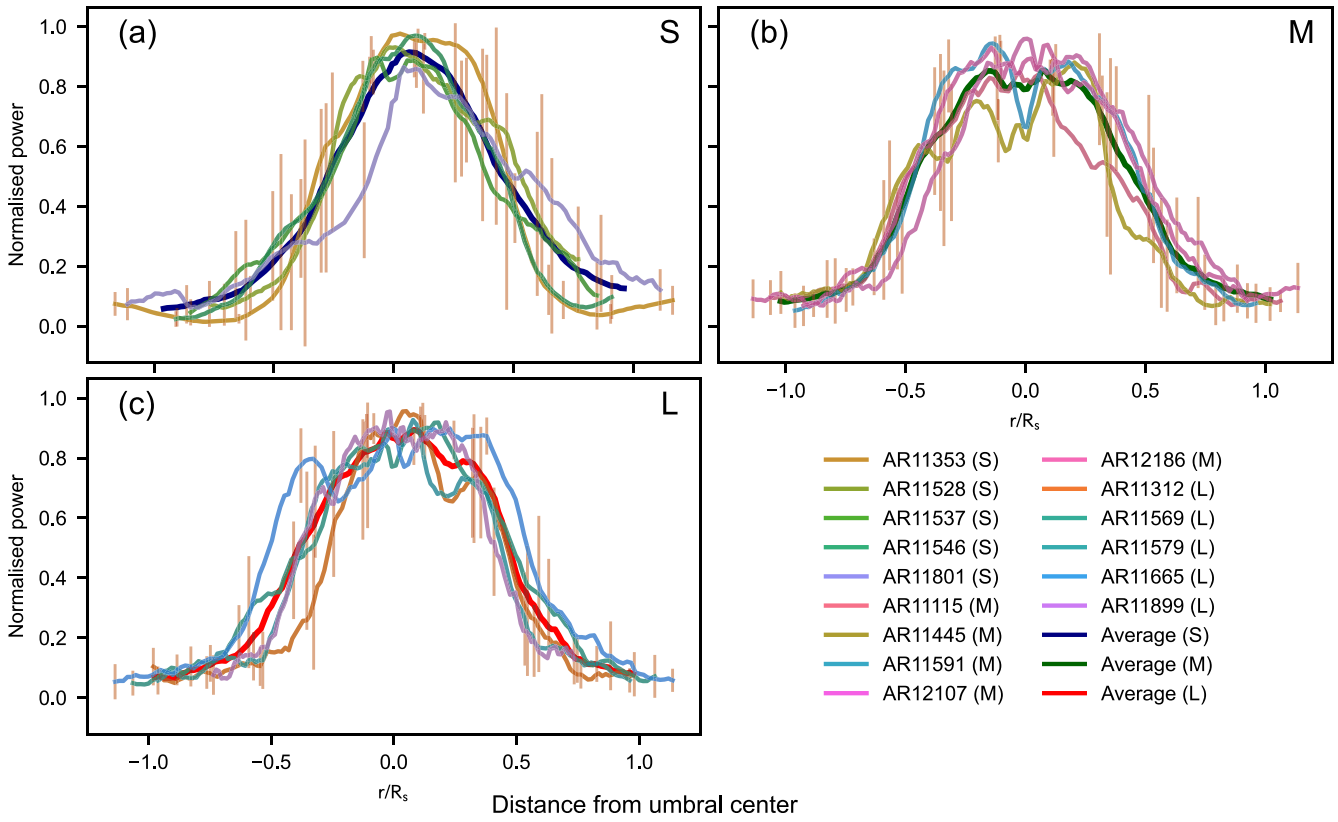

Figure 8. Three-minute narrowband power spectrum distribution, from SDO/AIA 1600 Å.

pronounced, which is probably attributed to the interaction of thermal and magnetic pressures.

4. Conclusion and Discussion

In this study, we analyzed the oscillations of 15 sunspots of different sizes using SDO/AIA data. This paper aimed to analyze and compare the periodic signals of sunspot emission intensity, obtain the spatial distribution of sunspot oscillation characteristics by spectrum analysis, explore the pattern of sunspot oscillation characteristics with sunspot magnetic field and thermodynamic structure by combining the variations of sunspot magnetic field with sunspot size, and develop tools for diagnosing the sunspot structure.

Our observations are as follows: (1) the three-minute oscillations are concentrated in the umbra, and the five-minute distribution is in the penumbra. (2) The sunspot umbra three-minute oscillations are present from the photosphere to the chromosphere, and the photosphere umbral oscillations are mixed by multiple wave modes and include one-minute oscillations. (3) The complexity of different sizes of the sunspot profile is different, and the analysis of the slice curve can reveal its structure.

The power distribution analysis reveals that in the upper photosphere, chromosphere, and transition region of sunspots, the power of three-minute oscillation is mainly concentrated in the sunspot umbra, whereas the power of five-minute oscillation is concentrated in the penumbra region. The region with strong oscillation power shows a nearly circular or ring-like structure. Along the magnetic line direction, sunspot oscillations are transmitted in the form of slow-mode magnetoacoustic waves, and the power distribution of the oscillations is basically unchanged in the solar atmosphere between the upper photosphere and the transition region; when the sunspot oscillations are transmitted to the corona, the power distribution of the oscillations starts to diverge. As shown by Reznikova & Shibasaki (2012) for the magnetic field structure, the cut-off frequency of the oscillations changes because of the change of the magnetic field inclination in the sunspots, resulting in the three-minute oscillations and five-minute oscillations being confined to the sunspot umbra and penumbra. The main reason for this is that the p-mode oscillations in the photosphere interact with the strong magnetic field in the sunspot when passing through the sunspot region, and the abrupt change at the umbra-penumbra boundary is likely to be caused by the effective absorption of the p-mode

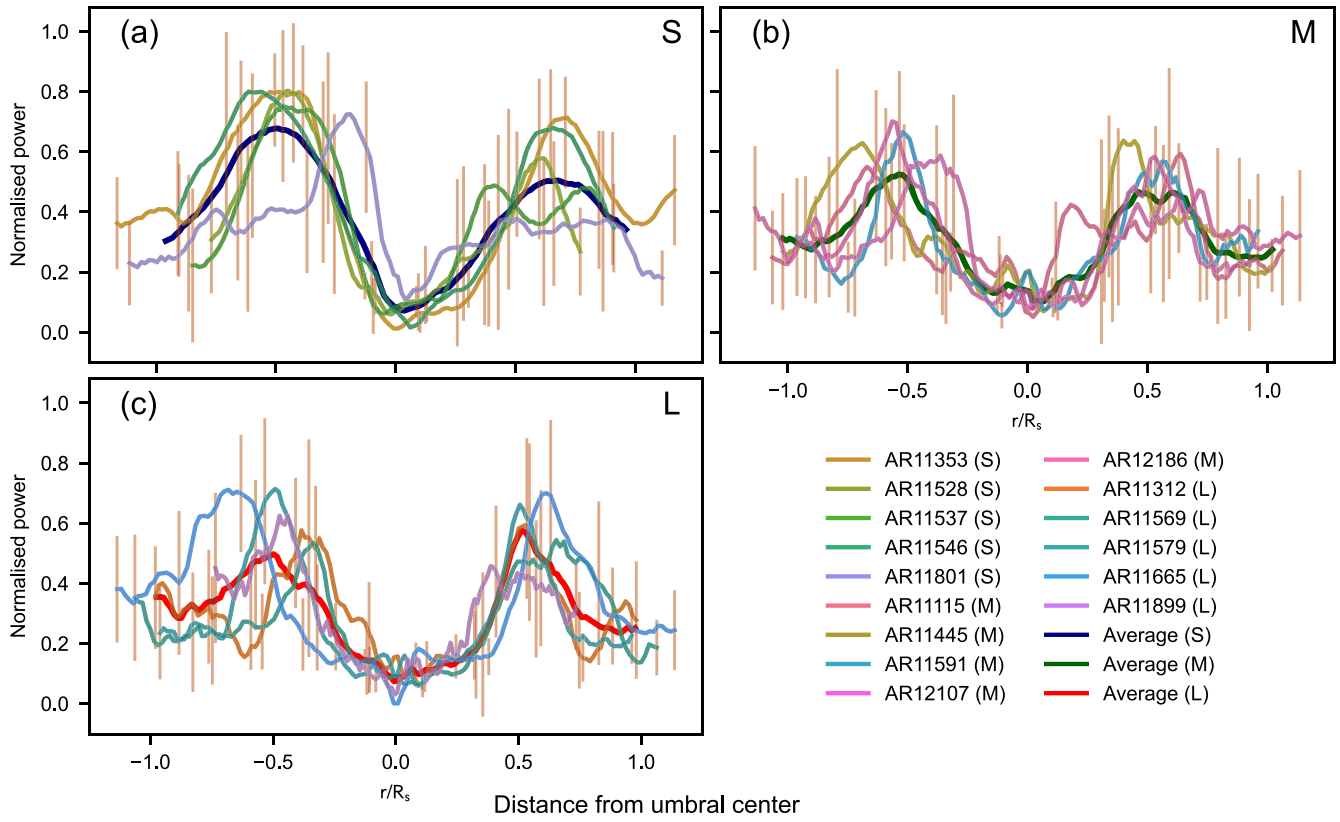

Figure 9. Five-minute power narrowband spectrum distribution, from SDO/AIA 1600 Å.

oscillations. Our conclusions are in agreement with Reznikova et al. (2012).

The distribution of the peak period demonstrates that the oscillations in the chromosphere umbra are dominated by the period of two to four minutes, which can be seen in the part of the sunspot umbra to the inner umbra where the period changes more flatly until the penumbra region where the peak period increases rapidly. From the AIA 1700 to 304 Å channels, the three-minute oscillation is constantly in existence, indicates that the three-minute oscillation originates in the photosphere and propagates upward (O'shea et al. 2002; Chae et al. 2017).

The region of the umbra-penumbra boundary occupied by the five-minute penumbra oscillation is likely a ring structure in the sunspots of different sizes. This outcome indicates that five-minute oscillations propagate along the inclined magnetic flux tube. Compared with the peak period in the chromosphere, the photosphere penumbra shows a mixture of multiple dominant wave periods, and a mixture of one minute, three minutes, and five minutes can be seen, with the one-minute peak period showing a dotted distribution in the umbra, the energy of these 1 minute oscillations may originate from deeper in the photosphere.

In AR11312 and AR11899, we can also see long-period oscillations in the umbra with a period of about 8 minutes, in contrast to Figures 3 and 4. We can find a spatial distribution of long-period oscillations in the umbra corresponding to the absence of the power distribution in the three-minute umbral oscillation and the distribution of power in the five-minute umbral oscillation. These structures found only in mature sunspots.

The slice analysis of the sunspot magnetic field and power distribution shows that the curve variation of small sunspots is relatively smoother. Because each slice is an average of the whole sunspot slice, it can only reflect the overall variation of the sunspot. By comparing and analyzing the difference between small, medium and large sunspots, it is found that the fine variation of sunspot magnetic field can change the peak period of sunspot oscillation, and such a correlation has the potential to explore the sunspot magnetic field and thermodynamic parameters.

In this research, we performed the statistical distribution of 15 sunspots and found some interesting phenomena. The structure of small sunspots is likely to be too small to find more useful information because of the lack of SDO spatial resolution, and some new instruments can help us to conduct more detailed studies, e.g., Goode Solar Telescope, European Solar Telescope, and so on. We will analyze the long-period oscillations in specific regions in sunspots afterward, and the oscillation pattern of multiple frequency mixing in the umbra of AR12384 will be further analyzed in the next study.

Acknowledgments

This study is supported by the National Natural Science Foundation of China (NSFC, Grant Nos. 12173012 and 12111530078) and the Shenzhen Technology project (GXWD20201230155427003-20200804151658001). S.F. is supported by the Joint Funds of the NSFC (U1931107).

ORCID iDs

Song Feng https://orcid.org/0000-0003-4709-7818

References

Bogdan, T., & Judge, P. 2006, RSPTA, 364, 313
Botha, G., Arber, T., Nakariakov, V., & Zhugzhda, Y. 2011, ApJ, 728, 84
Chae, J., Lee, J., Cho, K., et al. 2017, ApJ, 836, 18
De Moortel, I., Ireland, J., Hood, A., & Walsh, R. 2002, A&A, 387, L13
Khomenko, E., & Collados, M. 2006, ApJ, 653, 739
Khomenko, E., & Collados, M. 2015, LRSP, 12, 1
Kobanov, N., Chelpanov, A., & Kolobov, D. Y. 2013, A&A, 554, A146
Lemen, J. R., Akin, D. J., Boerner, P. F., et al. 2011, The Solar Dynamics Observatory (Berlin: Springer), 17
McIntosh, P. S. 1990, SoPh, 125, 251
O'shea, E., Muglach, K., & Fleck, B. 2002, A&A, 387, 642
Reznikova, V., & Shibasaki, K. 2012, ApJ, 756, 35
Reznikova, V., Shibasaki, K., Sych, R., & Nakariakov, V. 2012, ApJ, 746, 119
Scherrer, P. H., Schou, J., Bush, R., et al. 2012, SoPh, 275, 207
Sych, R., & Nakariakov, V. 2014, A&A, 569, A72
Wang, F., Deng, H., Li, B., et al. 2018, ApJL, 856, L16
Yuan, D., & Nakariakov, V. 2012, A&A, 543, A9
Yuan, D., Nakariakov, V. M., Huang, Z., et al. 2014a, ApJ, 792, 41
Yuan, D., Su, J., Jiao, F., & Walsh, R. W. 2016, ApJS, 224, 30
Yuan, D., Sych, R., Reznikova, V., & Nakariakov, V. 2014b, A&A, 561, A19
Yuan, D., & Walsh, R. W. 2016, A&A, 594, A101